After endarterectomy an expert (G.P.) blinded for the strain results classified the phenotype of the culprit lesion segment of the excised plaque following a validated histologic procedure (5). A plaque was classified as fibrous when it had no, or a small lipid core (10% of plaque area), low macrophage infiltration and high smooth muscle cell and collagen content, otherwise it was classified as (fibro)atheromatous.

The Elastin van Gieson-stained histology images and corresponding strain images of the cover figure illustrate that locally elevated strains were observed in atheromatous plaque regions, whereas strains were low for fibrous collagen-rich plaques. Strain parameter values were significantly higher (Mann-Whitney U test, $p < 0.01$) for (fibro)atheromatous plaques ($n = 20$; median 55.3% [interquartile range: 44.5% to 67.5%]) compared to fibrous plaques ($n = 14$; 34.5% [27.8% to 42.4%]), (**Figure 1**).

A limitation of this study is the relatively small sample size. Furthermore, because CUSI is ultrasound-based, acoustic shadowing impedes strain imaging in heavily calcified plaques. In this study only cases without severe shadowing and which cross section remained in the imaging plane from systole to diastole were included.

To conclude, CUSI was applied successfully in severely stenotic human carotid plaques and strain positively correlated with the presence of an atheromatous core. Because CUSI is relatively inexpensive, noninvasive, and patient-friendly, it might be the first technique to allow screening for vulnerable plaques in earlier (subclinical) stages of atherosclerosis and monitor individual plaque progression over time. Prospective studies such as ECST-2 (European Carotid Surgery Trial 2) have to demonstrate this.

Hendrik H.G. Hansen, PhD*
Gert Jan de Borst, MD, PhD
Michiel L. Bots, MD, PhD
Frans L. Moll, MD, PhD
Gerard Pasterkamp, MD, PhD
Chris L. de Korte, PhD

*Department of Radiology and Nuclear Medicine
Radboud University Medical Center
P.O. Box 9101
Geert Grooteplein-Zuid 10
Nijmegen, Gelderland 6500 HB
the Netherlands
E-mail: rik.hansen@radboudumc.nl

http://dx.doi.org/10.1016/j.jcmg.2016.05.008

Please note: Dr. de Korte has the same affiliation as the corresponding author and is in charge of the Medical UltraSound Imaging Center (MUSIC). Dr. de Borst is affiliated with the Department of Vascular Surgery of the University Medical Center Utrecht (the Netherlands) which is headed by Dr. Moll. Dr. Bots is in charge of the Julius Center for Health Sciences and Primary Care, and Dr. Pasterkamp is heading the Laboratory of Experimental Cardiology and Laboratory of Clinical Chemistry (research), both are also part of the University Medical Center Utrecht. This research (project number NKG 07589) is supported by the Dutch Technology Foundation (STW), which is part of the Netherlands Organization for Scientific Research (NWO), and is partly funded by the Ministry of Economic Affairs. The authors have reported that they have no relationships relevant to the contents of this paper to disclose.

REFERENCES

1. Hellings WE, Peeters W, Moll FL, et al. Composition of carotid atherosclerotic plaque is associated with cardiovascular outcome: a prognostic study. Circulation 2010;121:1941–50.

2. Schaar JA, de Korte CL, Mastik F, et al. Characterizing vulnerable plaque features by intravascular elastography. Circulation 2003;108:2636–41.

3. Hansen HHG, Lopata RGP, Idzenga T, de Korte CL. Full 2D displacement vector and strain tensor estimation for superficial tissue using beam-steered ultrasound imaging. Phys Med Biol 2010;55:3201–18.

4. Zervantonakis IK, Fung-Kee-Fung SD, Lee WN, Konofagou EE. A novel, view-independent method for strain mapping in myocardial elastography: eliminating angle and centroid dependence. Phys Med Biol 2007;52:4063–80.

5. Hellings WE, Pasterkamp G, Vollebregt A, et al. Intraobserver and interobserver variability and spatial differences in histologic examination of carotid endarterectomy specimens. J Vasc Surg 2007;46:1147–54.

Myocardial T2 Mapping Increases Noninvasive Diagnostic Accuracy for Biopsy-Proven Myocarditis

Detection of myocardial inflammation in patients with clinically suspected acute myocarditis (sAMC) is of prognostic importance but remains a challenge in routine clinical practice (1). Compared with endomyocardial biopsy (EMB), the diagnostic gold standard, cardiovascular magnetic resonance (CMR) offers the advantage of being readily available and omits the drawback of sampling errors (1). However, current Lake Louise Criteria for CMR-based diagnosis of myocarditis lack diagnostic accuracy due to inadequate negative predictive values (1). Recently, parametric CMR approaches, quantifying native T1 and T2 relaxation times without the need for contrast agents, have increased the diagnostic accuracy in patients with sAMC (2,3). Additionally, increased myocardial T2 values were shown to be associated with myocardial inflammation (4).

The aim of this prospective study was to further improve the diagnostic value of T2 mapping in patients with sAMC. We systematically applied T2 mapping (5) and right ventricular EMB whenever clinically feasible in patients presenting with sAMC. Following T2 mapping, we quantified the extent of myocardium with abnormal T2 time expressed as a percentage of whole myocardium. Patients with biopsy-proven acute myocarditis (bpAMC) served to determine the threshold of abnormal T2 time compared with a cohort of age- and sex-matched controls.

Sixty patients were recruited 3 ± 2 days after symptom onset and underwent CMR, including T2-

JACC: CARDIOVASCULAR IMAGING, VOL. 9, NO. 12, 2016
DECEMBER 2016:1466–76

FIGURE 1 The Extent of Myocardium With Pathological T2 Values Increases With the Extent of Inflammation and Offers Improved Diagnostic Accuracy in Detection of Myocarditis

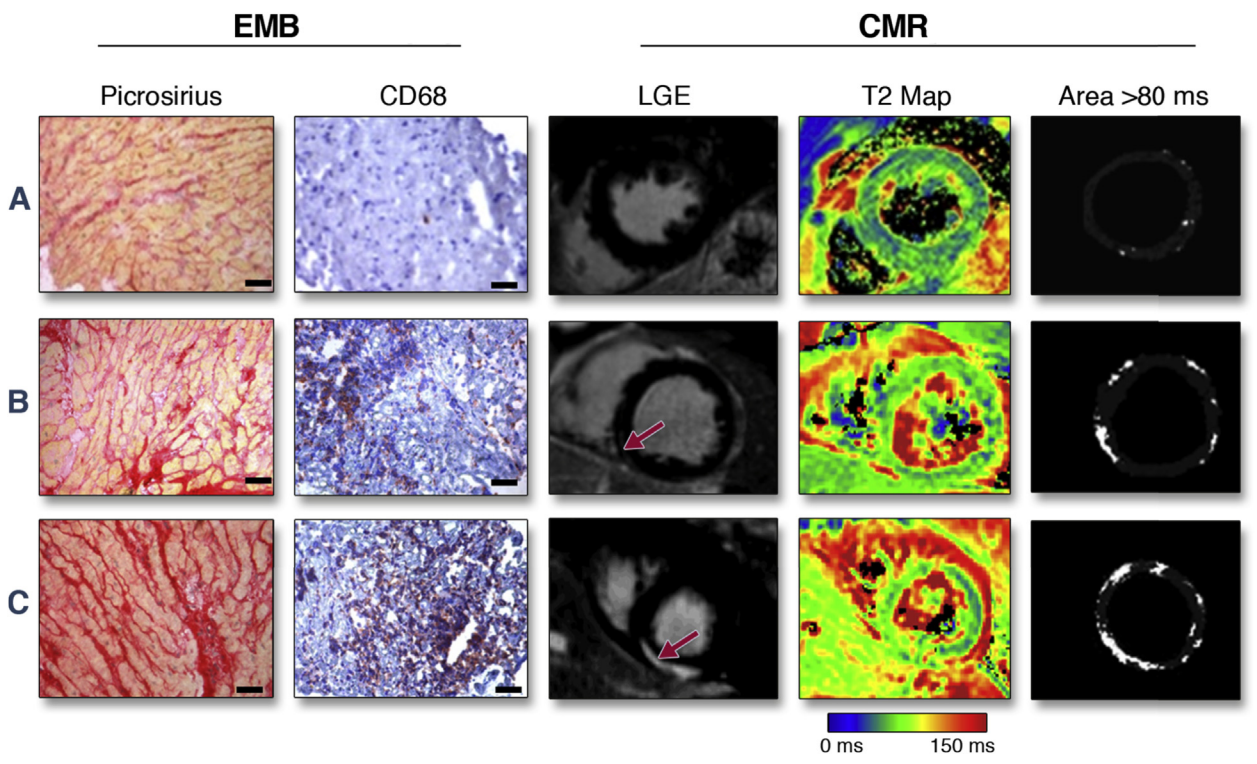

(A) A patient with exclusion of myocarditis. **(B)** Moderate myocardial inflammation, as shown by Picrosirius red and macrophage stain (CD68 positive [brown dots] >14 but <50 cells/mm^2). **(C)** Severe inflammation (CD86 positive >50 cells/mm^2). **Bar** = 50 μm. Late gadolinium enhancement (LGE) lesions are marked **(red arrows)**. T2 time in T2 maps is given in a color code ranging from 0 to 150 ms. Regions of interest for delineation of myocardial areas exceeding 80 ms (highlighted in **white**) are presented: patient A: 2.4%, patient B: 13%, and patient C: 39%.

weighted imaging and late gadolinium enhancement, and EMB within 48 h. Of 37 patients who received EMB, 26 were characterized as having bpAMC. In these selected patients with bpAMC, we detected a significant difference in average global myocardial T2 time compared with that of healthy volunteers (68.23 ± 6.4 ms vs. 60.11 ± 4.74 ms), confirming recent observations (4). However, there was a wide overlap of average T2 times in healthy volunteers and patients with bpAMC, thus hampering diagnosis of myocarditis by CMR. This overlap of average T2 time differences is due at least in part to the nature of myocarditis lesions being confined to small areas with abnormal T2 times compared with large areas of myocardium with normal T2 times, thereby blurring diagnostic accuracy (Figure 1). In the current study, we bypassed this shortcoming and quantified the extent of myocardium with abnormal T2 times (exceeding 80 ms) because 80 ms is rarely found in healthy volunteers (Figure 1). Applying this strategy, discrimination between patients with bpAMC and controls was markedly improved, with only marginal overlap between the groups (healthy vs. bpAMC 3.3 ± 2.7% vs. 14.68 ± 9.4%; $p < 0.001$) (Figure 1). Next we applied receiver-operating characteristic analysis to determine the optimal cutoff value to detect bpAMC by CMR with T2 mapping. We a priori defined the specificity to be 90%. receiver-operating characteristic analysis revealed that a myocardial extent of ≥7.6% with pathological T2 time detects bpAMC with a sensitivity of 92% ($p < 0.001$).

Quantitative analysis of myocardial inflammation in patients with bpAMC indicated that invasion of CD3- and CD68-positive cells coincides with the extent of myocardium with abnormal T2 times. Thus, patients presenting with myocardial inflammation and >50 CD3- or CD68-positive cells/mm^2 had >15% of myocardial areas exceeding 80 ms, whereas patients with <50 CD3- or CD68-positive cells/mm^2 had <15% with abnormal T2 times ($p < 0.05$).

In summary, the current study refined the observation of increased myocardial T2 times in patients

with bpAMC (4) toward a diagnostic tool with potential for CMR-based diagnosis of myocarditis in individual patients. The extent of myocardium with abnormal T2 times above 7.6% identifies bpAMC with a diagnostic accuracy of >90%. The prognostic meaning of elevated T2 in terms of functional recovery remains to be determined.

Florian Bönner, MD
Maximilian Spieker, MD
Sebastian Haberkorn, MD
Christoph Jacoby, PhD
Ulrich Flögel, PhD
Bernhard Schnackenburg, PhD
Patrick Horn, MD
Petra Reinecke, MD
Mirja Neizel-Wittke, MD
Malte Kelm, MD
Ralf Westenfeld, MD*

*Department of Medicine
University Hospital Duesseldorf, Medical Faculty
Division of Cardiology, Pulmonology and Vascular Medicine
Moorenstrasse 5
D-40225 Düsseldorf
Germany
E-mail: ralf.westenfeld@med.uni-duesseldorf.de

http://dx.doi.org/10.1016/j.jcmg.2015.11.014

Please note: Dr. Schnackenburg is employed by Philips Healthcare. All other authors have reported that they have no relationships relevant to the contents of this paper to disclose.

REFERENCES

1. Friedrich MG, Sechtem U, Schulz-Menger J, et al. Cardiovascular magnetic resonance in myocarditis: a JACC white paper. J Am Coll Cardiol 2009;53:1475–87.

2. Hinojar R, Foote L, Arroyo UE, et al. Native T1 in discrimination of acute and convalescent stages in patients with clinical diagnosis of myocarditis: a proposed diagnostic algorithm using CMR. J Am Coll Cardiol Img 2015;8:37–46.

3. Thavendiranathan P, Walls M, Giri S, et al. Improved detection of myocardial involvement in acute inflammatory cardiomyopathies using T2 mapping. Circ Cardiovasc Imaging 2012;5:102–10.

4. Bohnen S, Radunski UK, Lund GK, et al. Performance of T1 and T2 mapping cardiovascular magnetic resonance to detect active myocarditis in patients with recent-onset heart failure. Circ Cardiovasc Imaging 2015;8:e003073.

5. Bonner F, Janzarik N, Jacoby C, et al. Myocardial T2 mapping reveals age- and sex-related differences in volunteers. J Cardiovasc Magn Reson 2015;17:9.

Illustration of the Resorption Process Between 2 Different Overlapping Bioresorbable Scaffolds

A 65-year-old man with stable angina underwent percutaneous coronary intervention with a 3.0 × 18-mm bioresorbable scaffold (BRS) type 1 (DESolve, Elixir Medical Corp., Sunnyvale, California) in the mid-left anterior descending artery, followed by a 2.5 × 28-mm BRS type 2 (Absorb, Abbott Vascular, Santa Clara, California) to cover a distal edge dissection because another BRS type 1 could not pass distally. The final angiographic result was excellent (**Figures 1A and 1B**).

After 10 months, the patient presented with a recurrence of his anginal symptoms and underwent repeat coronary angiography. There was angiographic evidence of a significant restenosis at the overlapping site and throughout the BRS type 1 (**Figure 1C**). Optical coherence tomography (OCT) was performed and revealed significant neointimal hyperplasia at the sites. Furthermore, multiple overhung struts (discontinuities or strut fractures) were observed in BRS type 1; however, no discontinuity was present with BRS type 2 (**Figures 1D to 1H**).

Several types of BRS are in development (1), of which BRS type 1 and type 2 are the first 2 BRSs approved by the Conformité European mark for use in coronary artery disease. They have different bioresorption times: BRS type 2 completely resorbs within 3 years and BRS type 1 within 2 years. Late discontinuity is considered part of the normal bioresorption process (2) and is presumed to occur at different times as resorption rates vary between BRSs.

In this case, OCT was not performed at the index procedure; therefore, we were unsure whether the overhung struts were late discontinuities or strut fractures formed at the index procedure. If the latter is true, this could account for the difference in restenosis between the 2 types of scaffold. Furthermore, the overlapping site developed the most severe in-scaffold restenosis, which suggests that overlapping current-generation BRS, which have very thick struts, should be avoided and preference given to an abutting scaffold to scaffold strategy.

This case uniquely illustrates the differences in resorption process between the 2 commercially available BRS implanted in the same vessel.

Akihito Tanaka, MD*
Richard J. Jabbour, MD
Hiroyoshi Kawamoto, MD
Azeem Latib, MD
Antonio Colombo, MD

*EMO-GVM Centro Cuore Columbus
48 Via M. Buonarroti
20145 Milan
Italy
E-mail: info@emocolumbus.it

http://dx.doi.org/10.1016/j.jcmg.2015.12.013

Please note: Dr. Latib serves on the advisory board for Medtronic. All other authors have reported that they have no relationships relevant to the contents of this paper to disclose.